Available online at www.sciencedirect.com
ScienceDirect
Mathematics and Computers in Simulation 203 (2023) 669–684
MATHEMATICS AND COMPUTERS IN SIMULATION
www.elsevier.com/locate/matcom

Original articles

# Modelling and analysis of delayed tumour–immune system with hunting T-cells

Kaushik Dehingia[a,*,1], Parthasakha Das[b,*,1], Ranjit Kumar Upadhyay[c,1], Arvind Kumar Misra[d,1], Fathalla A. Rihan[e,1], Kamyar Hosseini[f,g,1]

[a] Department of Mathematics, Sonari College, Sonari 785690, Assam, India
[b] Department of Mathematics, Indian Institute of Engineering Science and Technology, Shibpur, Howrah, India
[c] Department of Mathematics & Computing, Indian Institute of Technology (Indian School of Mines), Dhanbad, India
[d] Department of Mathematics, Institute of Science, Banaras Hindu University, Varanasi, India
[e] Department of Mathematical Sciences, College of Science, United Arab Emirates University, 15551, Al-Ain, United Arab Emirates
[f] Department of Mathematics, Rasht Branch, Islamic Azad University, Rasht, Iran
[g] Department of Mathematics, Near East University TRNC, Mersin 10, Turkey

Received 27 January 2022; received in revised form 4 July 2022; accepted 7 July 2022
Available online 16 July 2022

**Abstract**

This study proposes a modified prey–predator-like model consisting of tumour cells, hunting T-cells, and resting T-cells to illustrate tumour–immune interaction by incorporating discrete-time-delay with conversion or growth of hunting cells. For analysis, the proposed system has been transformed into a normalized system, and its non-negativity solution has been verified. The linear stability of the system has been analysed at each equilibrium. The discrete-time delay affects the system's stability, and the system undergoes a Hopf bifurcation. Moreover, the length of time delay for which a periodic solution can be preserved has been derived. Finally, numerical computations have been presented that correlate with analytical results and are also relevant from a biological perspective.


*Keywords:* Tumour–immune interaction; Hunting T-cells; Time-delay; Hopf-bifurcation

## 1. Introduction

Nowadays, researchers are employing mathematical models to investigate how cancer grows under the influence of the immune system [3,7,9–11,14–16,20,29,31,40,43,44], and different treatment strategies [1,2,12,28,41,42,45]. Nevertheless, there has been an increasing interest in the role of the immune system in stopping tumour growth [30]. Cells such as macrophages, natural killer cells, and T-cells help the immune response fight against tumours. Kuznetsov et al. [27] proposed a mathematical model to show how the cytotoxic T-lymphocytes respond when an immunogenic tumour develops. They used a realistic set of parameter values for local and global bifurcations to

* Corresponding authors.
*E-mail addresses:* kaushikdehingia17@gmail.com (K. Dehingia), parthasakha87das@gmail.com (P. Das).
[1] All authors jointly worked on the results and they read and approved the final manuscript.

https://doi.org/10.1016/j.matcom.2022.07.009

predict tumour growth and clinical manifestations. By developing a mathematical model that could be tested in both mice and humans, de Pillis et al. [17] investigated the roles of natural killer (NK) and $CD8^+$ T-cells in suppressing various tumour cells. Rihan et al. [36] have modified the Kuznetsov et al. [27] model with the inclusion of adoptive cellular immunotherapy, and they explain the effectiveness of the prescribed therapy on the elimination process of the tumour. Dritschel et al. [21] investigated the role of cytotoxic and helper T-cells in eliminating cancerous tumours. They also demonstrated that combination therapies that stimulate the immune system while inhibiting tumour-induced immuno-suppression may synergistically slow cancer progression. Pang et al. [33] recently reported that increasing the flow of mature cytotoxic T-lymphocytes could eradicate tumour cells completely. Beck et al. [5] developed a mathematical model to describe the dynamic in vivo two-photon imaging of tumour-infiltrating CTLs and to determine the effects of $CD137$ agonist antibodies on their function. They found that the immediate effects of co-stimulation via the $CD137$ receptor were a more potent anti-proliferative effect with a more sustained presence of CTLs within the tumour.

It has been demonstrated by Bi et al. [6], Rihan et al. [35], Ghosh et al. [24], Dong et al. [19], Khajanchi et al. [26], Das et al. [8,13] Sardar et al. [38], Dehingia et al. [18] that the time-delay in tumour–immune dynamics is significant since it is incorporated as a memory effect in the biological systems [34]. Furthermore, several studies have reported that discrete-time lags considered in various processes such as the development and growth of cellular molecules, the proliferation of cells, stimulation of cell populations, differentiation of cell populations, and interaction between two cells describe a realistic scenario for tumour–immune dynamics. In this study, we developed a mathematical model based on three *delay differential equations* to model the dynamics of the tumour–immune system with hunting T-cells.

It is possible to distinguish between two types of T-cells: (i) cytotoxic T-lymphocytes or hunting T-cells, which are capable of killing tumours through direct interaction; and (ii) T-helper cells or resting T-cells, which are not capable of killing tumours through direct interaction but can aid in the action of hunting T-cells by secreting anti-tumour cytokines. In light of the preceding scenario, Sarkar and Banerjee [39] developed a prey–predator type deterministic tumour growth model in 2005 that took into account tumour cells, hunting T-cells, and resting T-cells. According to their findings, a threshold value for the rate of predation of tumour cells by the hunting cells can be determined by comparing the rate at which resting cells convert to hunting cells with the other system parameters at which the growth of the tumour can be controlled. The researchers also converted the deterministic model to a stochastic one by allowing random fluctuations to regression. As a result, they discovered specific conditions and threshold values for the intensities of stochastic fluctuations for which the density of malignant tumour cells decreases to a very low value. El-Gohary [22] extended the model [39] to a problem of optimal control for controlling the chaos in unstable steady-states of the system. It was revealed through the analyses that the system exhibits a transition from an uncontrolled to a controlled steady-state for a variety of parameter values and initial densities. Sarkar and Banerjee [39] model has been modified yet again in two different works [4,37], including time-delay. Because of time delay, the results of both studies revealed that stability switches to unstable via Hopf-bifurcation due to the disturbance caused by it. Based on the work [22,39], Kaur and Ahmad [25] developed a model which included the Michaelis–Menten function for the stimulation of resting cells by tumour cells. As a result of their findings, if the growth rate of resting cells increases, the immune system may prevent tumour cells from progressing. The model Kaur and Ahmad [25] is the foundation of our current research. Because the resting T-cells are converted to the hunting stage through various chemical processes, it is biologically plausible that the resting T-cells are not continuously converted to the hunting stage at the onset of the tumour. In this way, there is the possibility that hunting T-cells will grow at a slower rate than normal, a phenomenon known as conversion or growth delay. To this end, we introduce a discrete time-delay term into the growth process of hunting T-cells in the model of Kaur and Ahmad [25].

The organization of the remaining sections is as follows; the proposed model is presented in Section 2. We discuss the model's qualitative behaviour, such as positivity, the existence of equilibria, and linear stability, in Section 3. Section 4 examines the Hopf bifurcation and estimates the length of the time delay that is necessary to maintain stability. In Section 5, the findings of the analysis are validated numerically. Finally, in Section 6, some concluding remarks are presented.

## 2. Model description

In recent decades, the theoretical study of tumour–immune dynamics has become a rising trend. As a result, various mathematical models have been developed to address different aspects of tumour–immune dynamics. A

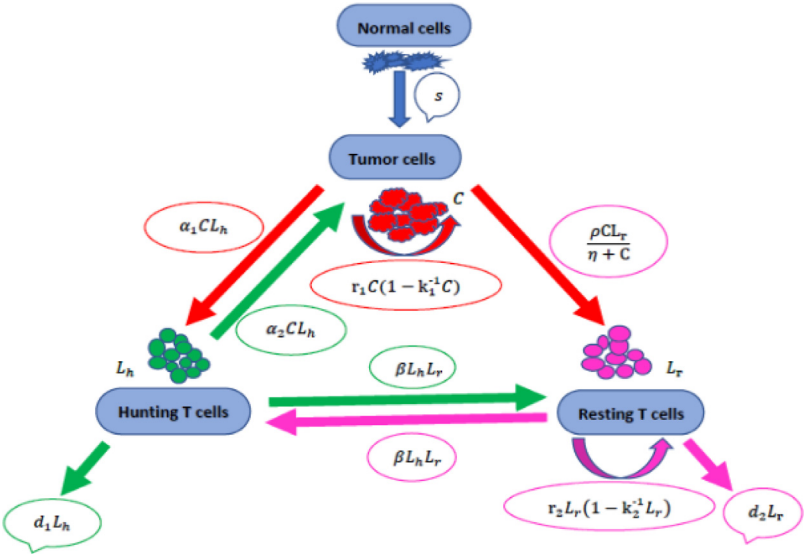


**Fig. 1.** The schematic diagram of the model consisting of tumour cells ($C$), Hunting T-cells ($L_h$) and resting T-cells ($L_r$).

modified version of the Kaur and Ahmad [25] model has been proposed in this study, with a discrete-time delay in the growth of hunting T-cells as an intervention. So, the proposed model takes the following form:

$$\left.\begin{aligned}
\frac{dC(\tau)}{d\tau} &= s + r_1 C(\tau)(1 - k_1^{-1} C(\tau)) - \alpha_1 C(\tau) L_h(\tau), \\
\frac{dL_h(\tau)}{d\tau} &= \beta L_h(\tau - \Delta) L_r(\tau - \Delta) - d_1 L_h(\tau) - \alpha_2 L_h(\tau) C(\tau), \\
\frac{dL_r(\tau)}{d\tau} &= r_2 L_r(\tau)(1 - k_2^{-1} L_r(\tau)) - \beta L_h(\tau) L_r(\tau) - d_2 L_r(\tau) + \frac{\rho C(\tau) L_r(\tau)}{\eta + C(\tau)},
\end{aligned}\right\} \tag{2.1}$$

where at any time $\tau$, $C(\tau)$ is the amount of malignant tumour cells, $L_h(\tau)$ is the amount of hunting T-cells and $L_r(\tau)$ is the amount of resting T-cells. The discrete-time delay in the growth of hunting T-cells is represented by $\Delta$. It is assumed that in the presence of tumour cells, the tumour-specific resting T-cells can grow, and this mechanism is represented by the Michaelis–Menten term $\frac{\rho C(\tau) L_r(\tau)}{\eta + C(\tau)}$, where $\rho$ is proliferation rate and $\eta$ is the steepness coefficient. The definitions of other parameters are as follows:

$s$: constant conversion rate of normal cells to malignant tumour cells.
$r_1$: growth rate of malignant tumour cells.
$k_1$: maximum carrying capacity of malignant tumour cells.
$\alpha_1$: killing rate of malignant tumour cells by hunting T-cells.
$\beta$: rate of conversion of the resting T-cells to hunting T-cells.
$d_1$: rate of natural decay of hunting T-cells.
$\alpha_2$: killing rate of hunting T-cells by malignant tumour cells.
$r_2$: growth rate of resting T-cells.
$d_2$: rate of natural decay of resting T-cells.

A schematic diagram of the model is shown in Fig. 1.

We convert the above system (2.1) into a dimensionless form by assuming $\left[x(t), y(t), z(t)\right] = \left(k_1^{-1}C, \alpha_1 k_1 s^{-1} L_h, k_2^{-1} L_r\right)$ with $t = s\tau k_1^{-1}$, $\delta = \Delta$, and the system takes the following form

$$\left.\begin{aligned} \frac{dx}{dt} &= 1 + a_1 x(1-x) - xy, \\ \frac{dy}{dt} &= a_2 y(t-\delta) z(t-\delta) - a_3 y - a_4 xy, \\ \frac{dz}{dt} &= a_5 z(1-z) - a_6 yz - a_7 z + \frac{a_8 xz}{K+x}, \end{aligned}\right\} \tag{2.2}$$

where $x(t)$, $y(t)$ and $z(t)$ respectively represent the normalized amount of malignant tumour cells, hunting T-cells and resting T-cells at any time $t$ with the new parameter set: $a_1 = r_1 k_1 s^{-1}$, $a_2 = \beta k_1 k_2 s^{-1}$, $a_3 = k_1 d_1 s^{-1}$, $a_4 = \alpha_2 k_1^2 s^{-1}$, $a_5 = r_2 k_1 s^{-1}$, $a_6 = \beta \alpha_1^{-1}$, $a_7 = k_1 d_2 s^{-1}$, $a_8 = k_1 \rho s^{-1}$, and $K = \eta k_1^{-1}$.

The history functions for the system (2.2) are:

$$x(\phi) = \psi_1(\phi),\ y(\phi) = \psi_2(\phi),\ z(\phi) = \psi_3(\phi), \tag{2.3}$$

with $\psi_1(\phi) \geq 0$, $\psi_2(\phi) \geq 0$ and $\psi_3(\phi) \geq 0$ for $\phi \in [-\delta, 0]$, where $\psi_i(\phi) \in \mathbb{R}_+$, $\forall i = 1, 2, 3$ and are the continuous mapping on $[-\delta, 0)$ which may display jumps at $\phi = 0$.

## 3. Qualitative behaviour

From the biological point of view, the proposed system (2.2) has to be a unique and non-negative solution corresponding to the history functions (2.3). In order to do, we state the following theorem.

### 3.1. Basic characteristics

**Theorem 3.1.** *Corresponding to the history functions (2.3), every solution of the system (2.2) is unique in* $[0, \infty)$ *and non-negative throughout the region* $\mathbb{R}^3_+$, *for all* $t > 0$.

**Proof.** The system (2.2) can be represented in vector form as $\dot{Z}(t) = \mathcal{A}(Z)$ where $Z = [x(t), y(t), z(t)]^T \in \mathbb{R}^3_{+,0}$, and the mapping $\mathcal{A} : \mathbb{C}_+ \mapsto \mathbb{R}^3_{+,0}$ for $\mathcal{A} \in C^\infty(\mathbb{R}^3_+)$ defined in the non-negative octant $\mathbb{R}^3_{+,0}$ where

$$\mathcal{A}(Z) = \begin{pmatrix} \mathcal{A}_1(Z) \\ \mathcal{A}_2(Z) \\ \mathcal{A}_3(Z) \end{pmatrix} = \begin{pmatrix} 1 + a_1 x(1-x) - xy \\ a_2 y(t-\delta) z(t-\delta) - a_3 y - a_4 xy \\ a_5 z(1-z) - a_6 yz - a_7 z + \frac{a_8 xz}{K+x} \end{pmatrix}. \tag{3.1}$$

The vector function $\mathcal{A}$ is locally Lipschitz and a continuous function, and it satisfies the conditions

$$\mathcal{A}_i(Z)|_{Z_i(t)},\ Z \in \mathbb{R}^3_+ = \mathcal{A}_i(0) \geq 0\ \forall\ i = 1, 2, 3. \tag{3.2}$$

Thus, for the history functions (2.3), $\psi_i(t) \in \mathbb{R}_+$, every solution of the system (2.2) is unique and it remains non-negative throughout the region $\mathbb{R}^3_+$, $\forall t > 0$ [43]. □

### 3.2. Equilibrium and linear stability

For $\delta = 0$, Kaur and Ahmad [25] already reported the linear stability conditions for the biologically feasible equilibrium of the system (2.2). However, the conditions of existence for the equilibrium of a time-delayed system are the same as for an ordinary system. Here, we will examine the stability of the systems' (2.2) at three biologically feasible equilibrium points.

- The equilibrium $E_1(x_1, 0, 0)$ with $x_1 = \frac{1}{2}(1 + \sqrt{1 + \frac{4}{a_1}})$ always exists. At this equilibrium, only malignant tumour cells are present, and it can be regarded as tumour-persistent equilibrium.
- The equilibrium $E_2(x_2, 0, z_2)$ with $x_2 = \frac{1}{2}\left(1 + \sqrt{1 + \frac{4}{a_1}}\right)$ and $z_2 = \frac{1}{a_5}\left(a_5 - a_7 + \frac{a_8 x_2}{K + x_2}\right)$ exists for $a_5 + \frac{a_8 x_2}{K + x_2} > a_7$. It implies that if the growth rate is greater than the death rate of resting $T$ cells in the presence of tumour cells, the equilibrium $E_2$ exists. At this equilibrium, only tumour and resting predator cells are present. This equilibrium is also regarded as tumour-persistent equilibrium.

- It is clear that the equilibrium $E^*(x^*, y^*, z^*)$ exists and is biologically feasible for $x^* > 0$, $y^* > 0$ and $z^* > 0$. It also exists only for $z^* = \frac{a_3+a_4x^*}{a_2}$, $y^* = \frac{a_5(1-\frac{a_3+a_4x^*}{a_2})-a_7+\frac{a_8x^*}{K+x^*}}{a_6}$ with the following equation

$$l_3x^{*3} + l_2x^{*2} + l_1x^* + l_0 = 0,$$

having at least one positive root $x^*$; where

$$\begin{aligned}
l_3 &= a_1a_0 - \frac{a_4a_5}{a_2},\\
l_2 &= a_5 - a_7 + a_8 - \frac{a_5}{a_2}(a_3 + a_4K) - a_1a_6(1 - K),\\
l_1 &= a_5K - \Big\{a_7K + \frac{a_5a_3K}{a_2} + a_6(a_1K + 1)\Big\},\\
l_0 &= -a_6K < 0.
\end{aligned}$$

Since, $l_0 < 0$ which guarantees that for $l_1 > 0, l_2 > 0, l_3 > 0$, there exists a positive real root $x^*$. At the equilibrium $E^*$, all three cells exists and it is regarded as an interior equilibrium.

In order to check the linear stability of the system (2.2) we use the classical Jacobian matrix and eigenvalues concepts. The Jacobian matrix for the system (2.2) is given by

$$\mathcal{V}_E = \begin{pmatrix} v_{11} & v_{12} & 0 \\ v_{21} & v_{22} & v_{23} \\ v_{31} & v_{32} & v_{33} \end{pmatrix}, \tag{3.3}$$

where $v_{11} = a_1 - 2a_1x - y$, $v_{12} = -x$, $v_{21} = -a_4y$, $v_{22} = a_2ze^{-m\delta} - a_3 - a_4x$, $v_{23} = a_2ye^{-m\delta}$, $v_{31} = \frac{a_8zK}{(K+x)^2}$, $v_{32} = -a_6z$, and $v_{33} = a_5 - 2a_5z - a_6y - a_7 + \frac{a_8x}{K+x}$.

I. The eigenvalues of (3.3) corresponding to $E_1$ are $m_1^1 = -\sqrt{1 + \frac{4}{a_1}}(< 0)$, $m_2^1 = -a_3 - \frac{a_4}{2}(1 + \sqrt{1 + \frac{4}{a_1}})(< 0)$, and $m_3^1 = a_5 - a_7 + \frac{\frac{a_8}{2}(1+\sqrt{1+\frac{4}{a_1}})}{\frac{1}{2}(1+\sqrt{1+\frac{4}{a_1}})+K}(> 0)$ as $a_5 > a_7$. Hence, the tumour-persistent equilibrium $E_1(x_1, 0, 0)$ with $x_1 = \frac{1}{2}(1 + \sqrt{1 + \frac{4}{a_1}})$ is always a saddle point.

II. At the tumour-persistent equilibrium point $E_2$, the eigenvalues of (3.3) are $m_1^2 = -\sqrt{1 + \frac{4}{a_1}}(< 0)$, $m_2^2 = -a_5 - 2a_5z_2 - a_7 + \frac{a_8x_2}{K+x_2}$, and $m_3^2 = a_2z_2 - a_3 - a_4x_2$. The equilibrium $E_2$ is locally asymptotically stable if $m_2^2 < 0 \implies a_2z_2 < a_3 + a_4x_2$ and $m_3^2 < 0 \implies \frac{a_8x_2}{K+x_2} < a_5 + 2a_5z_2 + a_7$.

III. It is already reported in [25] that the interior equilibrium $E^*$ is globally asymptotically stable in the interior of the positive octant of $THR$ space in the absence of discrete-time delay, i.e., $\delta = 0$. Now, we will explore the effect of discrete-time lag on the system (2.2) when all three cells co-exist, i.e., the dynamical behaviour of system (2.2) around the interior equilibrium $E^*(x^*, y^*, z^*)$. For the case of discrete-time lag $\delta \neq 0$, the characteristic equation of the linearized system around $E^*(x^*, y^*, z^*)$ can be written as

$$P(m) + Q(m)e^{-m\delta} = 0, \tag{3.4}$$

where

$$\left.\begin{aligned} P(m) &= m^3 + p_1m^2 + p_2m + p_3,\\ Q(m) &= q_1m^2 + q_2m + q_3, \end{aligned}\right\}$$

with

$$\left.\begin{aligned}
p_1 &= 2a_1x^* - a_1 + y^* + a_3 + a_4x^* - a_5 + 2a_5z^* + a_6y^* + a_7 - \frac{a_8x^*}{K+x^*},\\
p_2 &= (a_1 - 2a_1x^* - y^*)\big(a_5 - a_3 - a_4x^* - 2a_5z^* - a_6y^* - a_7 + \frac{a_8x^*}{K+x^*}\big)\\
&\quad - \big(a_5 - 2a_5z^* - a_6y^* - a_7 + \frac{a_8x^*}{K+x^*}\big)(a_3 + a_4x^*) - a_4x^*y^*,\\
p_3 &= (a_1 - 2a_1x^* - y^*)(a_3 + a_4x^*)\big(a_5 - 2a_5z^* - a_6y^* - a_7 + \frac{a_8x^*}{K+x^*}\big)\\
&\quad + a_4x^*y^*\big(a_5 - 2a_5z^* - a_6y^* - a_7 + \frac{a_8x^*}{K+x^*}\big),\\
q_1 &= -a_2z^*,\\
q_2 &= (a_1 - 2a_1x^* - y^*)a_2z^* + \big(a_5 - 2a_5z^* - a_6y^* - a_7 + \frac{a_8x^*}{K+x^*}\big)a_2z^* + a_2a_6y^*z^*,\\
q_3 &= a_2a_8x^*y^*z^*\frac{K}{(x^*+K)^2} - a_2z^*(a_1 - 2a_1x^* - y^*)(a_5 - 2a_5z^* - a_6y^* - a_7 + \frac{a_8x^*}{K+x^*})\\
&\quad - (a_1 - 2a_1x^* - y^*)a_2a_6y^*z^*.
\end{aligned}\right\}$$

In absence of time lag ($\delta = 0$), the characteristic Eq. (3.4) corresponds to interior equilibrium $E^*$ becomes

$$m^3 + (p_1 + q_1)m^2 + (p_2 + q_2)m + (p_3 + q_3) = 0, \tag{3.5}$$

where

$$\left.\begin{aligned}
p_1 &= 2a_1x^* - a_1 + y^* + a_2z^* + a_5z^*,\\
p_2 &= -(a_1 - 2a_1x^* - y^*)(a_2z^* + a_5z^*) + a_2a_5z^{*2} - a_4x^*y^*,\\
p_3 &= -(a_1 - 2a_1x^* - y^*)(a_2a_5z^{*2}) - a_4a_5x^*y^*z^*,\\
q_1 &= -a_2z^*,\\
q_2 &= (a_1 - 2a_1x^* - y^*)a_2z^* - a_2a_5z^{*2} + a_2a_6y^*z^*,\\
q_3 &= a_2a_8x^*y^*z^*\frac{K}{(x^*+K)^2} + a_2z^*(a_1 - 2a_1x^* - y^*)(a_5z^* - a_6y^*).
\end{aligned}\right\}$$

The Routh–Hurwitz criterion states that $E^*$ is asymptotically stable if the roots of the characteristic Eq. (3.5) are negative or have negative real parts, i.e., for $\chi_1 = p_1 + q_1 > 0$, $\chi_2 = p_3 + q_3 > 0$, and $\chi_3 = \chi_1(p_2 + q_2) - \chi_2 > 0$, equilibrium $E^*$ is asymptotically stable.
Therefore,

$$\begin{aligned}
\chi_1 &= 2a_1x^* - a_1 + y^* + a_2z^* + a_5z^* - a_2z^* > 0,\\
\chi_2 &= a_2a_8x^*y^*z^*\frac{K}{(x^*+K)^2} + a_2z^*(a_1 - 2a_1x^* - y^*)(a_5z^* - a_6y^*) - (a_1 - 2a_1x^* - y^*)(a_2a_5z^{*2})\\
&\quad - a_4a_5x^*y^*z^* > 0,\\
\chi_3 &= \big[2a_1x^* - a_1 + y^* + a_2z^* + a_5z^* - a_2z^*\big]\big[(a_1 - 2a_1x^* - y^*)a_2z^* - a_2a_5z^{*2} + a_2a_6y^*z^*\\
&\quad - (a_1 - 2a_1x^* - y^*)(a_2z^* + a_5z^*) + a_2a_5z^{*2} - a_4x^*y^*\big] - \big[a_2a_8x^*y^*z^*\frac{K}{(x^*+K)^2}\\
&\quad + a_2z^*(a_1 - 2a_1x^* - y^*)(a_5z^* - a_6y^*) - (a_1 - 2a_1x^* - y^*)(a_2a_5z^{*2})\\
&\quad - a_4a_5x^*y^*z^*\big] > 0.
\end{aligned}$$

Now, we will explore the discrete-time delay ($\delta \neq 0$) effect on the system (2.2). First, we will investigate the switching nature of systems' stability due to the presence of discrete-time lag $\delta$. In order to examine whether there exists a periodic solution or not for the system (2.2) considering $\delta$ as the bifurcating parameter, we substitute $m = \iota\omega$ ($\omega > 0$) into (3.4) and by separating the imaginary and real parts, we get

$$\left.\begin{aligned}
\omega^3 - p_2\omega &= q_2\omega\cos(\omega\delta) - (q_3 - q_1\omega^2)\sin(\omega\delta),\\
p_1\omega^2 - p_3 &= (q_3 - q_1\omega^2)\cos(\omega\delta) + q_2\omega\sin(\omega\delta),
\end{aligned}\right\} \tag{3.6}$$

For computing $\omega$, we square both sides of (3.6) and add the equations. This yields

$$\omega^6 + \kappa_1\omega^4 + \kappa_2\omega^2 + \kappa_3 = 0, \tag{3.7}$$

where

$$\left.\begin{aligned}
\kappa_1 &= p_1^2 - 2p_2 - q_1^2 \\
&= \left[2a_1x^* - a_1 + y^* + a_3 + a_4x^* - a_5 + 2a_5z^* + a_6y^* + a_7 - \frac{a_8x^*}{K+x^*}\right]^2 \\
&- 2\left[(a_1 - 2a_1x^* - y^*)\Big(a_5 - a_3 - a_4x^* - 2a_5z^* - a_6y^* - a_7 + \frac{a_8x^*}{K+x^*}\Big)\right. \\
&\left. - \Big(a_5 - 2a_5z^* - a_6y^* - a_7 + \frac{a_8x^*}{K+x^*}\Big)(a_3 + a_4x^*) - a_4x^*y^*\right] - [a_2z^*]^2, \\
\kappa_2 &= p_2^2 - 2p_1p_3 + 2q_1q_3 - q_2^2, \\
\kappa_3 &= p_3^2 - q_3^2.
\end{aligned}\right\}$$

From our general observation, it is obvious that for $\kappa_1 > 0$ and $\kappa_3 < 0$, Eq. (3.7) will have a positive root. From the above conditions, it is obvious that there is a unique non-negative root $\omega_0$ satisfying Eq. (3.7), i.e., the characteristic polynomial (3.4) has a pair of purely imaginary roots in the form $\pm\iota\omega_0$. Solving both the equations of (3.6), we have

$$\tan(\omega\delta) = \frac{q_2\omega(p_1\omega^2 - p_3) - (\omega^3 - p_2\omega)(q_3 - q_1\omega^2)}{(p_1\omega^2 - p_3)(q_3 - q_1\omega^2) + q_2\omega(\omega^3 - p_2\omega)}.$$

Then,

$$\delta_f = \frac{1}{\omega_0}\arctan\left[\frac{q_2\omega_0(p_1\omega_0^2 - p_3) - (\omega_0^3 - p_2\omega_0)(q_3 - q_1\omega_0^2)}{(p_1\omega_0^2 - p_3)(q_3 - q_1\omega_0^2) + q_2\omega_0(\omega_0^3 - p_2\omega_0)}\right] + \frac{2f\pi}{\omega_0}, \quad f = 0, 1, 2, 3, \ldots \tag{3.8}$$

For $\delta_f = 0$, the interior equilibrium point $E^*$ is locally asymptotically stable, provided $\chi_1 = p_1 + q_1 > 0$, $\chi_2 = p_3 + q_3 > 0$, and $\chi_3 = \chi_1(p_2 + q_2) - \chi_2 > 0$. Hence, by the well-known Butler's lemma, $E^*$ will remain stable for $0 < \delta < \delta_0$, where $\delta_f = \delta_0$ at $f = 0$. This implies that once the time delay traverses a given threshold value, the immune system will not be able to control the tumour cell growth. As a result, the patient's body begins to lose stability with the fast proliferation of malignant tumour cells.

## 4. Hopf bifurcation analysis

In this section, we will first derive the transversality conditions $\frac{d(Re(m))}{d\delta}|_{\delta=\delta_f} > 0$ for Hopf bifurcation of (2.2) at $\delta = \delta_0$ such that Eq. (3.4) has a pair of purely imaginary roots. For this, we have to establish the direction of motion of $\delta$ when $\delta_f$ is increased and hence we need to evaluate the following expressions:

$$\Phi = \text{sign}\left[\frac{d(Re(m))}{d\delta_f}\right]_{m=\iota\omega_0} = \text{sign}\left[Re\left(\frac{d(m)}{d\delta_f}\right)^{-1}\right]_{m=\iota\omega_0}.$$

**Theorem 4.1.** *For the system (2.2), if the interior equilibrium $E^*$ exists then*

*(i) for $\delta \in [0, \delta_0)$, $E^*$ is asymptotically stable,*
*(ii) $E^*$ is unstable if $\delta > \delta_0$,*
*(iii) $E^*$ undergoes Hopf bifurcation around $E^*$ if $\delta = \delta_0$.*

**Proof.** Differentiation of (3.4) with respect to $\delta$ leads to

$$[(3m^2 + 2p_1m + p_2) + (2q_1m + q_2)e^{-m\delta_f} - (q_1m^2 + q_2m + q_3)\delta e^{-m\delta_f}]\frac{d(m)}{d\delta_f} = me^{-m\delta_f}(q_1m^2 + q_2m + q_3),$$

which implies

$$\left[\frac{d(m)}{d\delta_f}\right]^{-1} = \frac{2m^3 + p_1m^2 - p_3}{-m^2(m^3 + p_1m^2 + p_2m + p_3)} + \frac{q_1m^2 - q_3}{m^2(q_1m^2 + q_2m + q_3)} - \frac{\delta_f}{m}.$$

Thus,

$$\begin{aligned}\Phi =& \text{sign}\left[Re\left(\frac{2m^3 + p_1m^2 - p_3}{-m^2(m^3 + p_1m^2 + p_2m + p_3)} + \frac{q_1m^2 - q_3}{m^2(q_1m^2 + q_2m + q_3)} - \frac{\delta_f}{m}\right)\right] \\ =& \frac{1}{\omega_0^2}\text{sign}\left[\frac{(p_1\omega_0^2 + p_3)(p_1\omega_0^2 - p_3) + 2\omega_0^3(\omega_0^3 - p_2\omega_0) + (q_1\omega_0^2 + q_3)(q_3 - q_1\omega_0^2)}{q_2^2\omega_0^2 + (q_3 - q_1\omega_0^2)^2}\right] \\ =& \frac{1}{\omega_0^2}\text{sign}\left[\frac{2\omega_0^6 + \omega_0^4(p_1^2 - 2p_2 - q_1^2) + (q_3^2 - p_3^2)}{q_2^2\omega_0^2 + (q_3 - q_1\omega_0^2)^2}\right].\end{aligned}$$

Therefore, the transversality condition $\frac{d(Re(m))}{d\delta}|_{\delta=\delta_f,\omega=\omega_0} > 0$ holds as $p_1^2 - 2p_2 - q_1^2 > 0$ and $q_3^2 - p_3^2 > 0$ by virtue of $\kappa_1 > 0$ and $\kappa_3 > 0$. It indicates that the stability switches from stable to unstable through a Hopf bifurcation $\delta = \delta_f = \delta_0$. Hence, we can report that the stability of our considered tumour-immune model is significantly affected by the discrete-time delay $\delta \neq 0$. The stable interior equilibrium $E^*$ where all the three cells exist, loses its stable nature because of the appearance of Hopf bifurcation at $\delta = \delta_0$ and becomes unstable for $\delta > \delta_0$ when we varied the parameter $\delta$. □

In the above, we already reported that the system (2.2) has a periodic solution. Here, we investigate whether the bifurcating periodic solution is stable or not; and if stable, we will compute the length of time lag for preserving the limit cycle's stability. First, we linearize the system (2.2) around the interior equilibrium $E^*(x^*, y^*, z^*)$, which gives us

$$\left.\begin{aligned}\frac{dx}{dt} &= (a_1 - 2a_1x^* - y^*)x - x^*y, \\ \frac{dy}{dt} &= -a_4y^*x + a_2z^*y(t-\delta) - (a_3 + a_4x^*)y + a_2y^*z(t-\delta), \\ \frac{dz}{dt} &= \frac{a_8z^*K}{(K+x^*)^2}x - a_6z^*y + (a_5 - 2a_5z^* - a_6y^* - a_7 + \frac{a_8x^*}{K+x^*})z.\end{aligned}\right\} \tag{4.1}$$

Taking Laplace transformation of (4.1), we get

$$\left.\begin{aligned}(\zeta + y^* + 2a_1x^* - a_1)\mathcal{S}_x(\zeta) &= -x^*\mathcal{S}_y(\zeta) + \bar{x}(0), \\ (\zeta + a_3 + a_4x^* - a_2z^*e^{-\zeta\delta})\mathcal{S}_y(\zeta) &= -a_4y^*\mathcal{S}_x(\zeta) + a_2y^*e^{-\zeta\delta}\mathcal{S}_z(\zeta) + \\ &\quad a_2y^*e^{-\zeta\delta}\mathcal{F}_z(\zeta) + a_2z^*e^{-\zeta\delta}\mathcal{F}_y(\zeta) + \bar{y}(0), \\ (\zeta + 2a_5z^* + a_6y^* + a_7 - a_5 - \frac{a_8x^*}{K+x^*})\mathcal{S}_z(\zeta) &= \frac{a_8z^*K}{(K+x^*)^2}\mathcal{S}_x(\zeta) - a_6z^*\mathcal{S}_y(\zeta) + \bar{z}(0),\end{aligned}\right\}$$

where $\mathcal{S}_x(\zeta)$, $\mathcal{S}_y(\zeta)$, and $\mathcal{S}_z(\zeta)$ are the Laplace transformation of $x(t)$, $y(t)$ and $z(t)$ respectively. Also, $\mathcal{F}_y(\zeta) = \int_{-\delta}^{0} e^{-\zeta t}y(t)dt$, and $\mathcal{F}_z(\zeta) = \int_{-\delta}^{0} e^{-\zeta t}z(t)dt$.

According to Freedman et al. [23] and classical Nyquist criteria [32], the interior equilibrium $E^*$ is asymptotically stable for

$$Re[H(\iota\mu_0)] = 0, \tag{4.2}$$

$$Im[H(\iota\mu_0)] > 0, \tag{4.3}$$

with

$$H(\zeta) = \zeta^3 + p_1\zeta^2 + p_2\zeta + p_3 + e^{-\zeta\delta}(q_1\zeta^2 + q_2\zeta + q_3),$$

and $\mu_0 > 0$ is the minimal non-negative root of the above expressions (4.2) and (4.3).

The explicit form of expressions (4.2) and (4.3) are

$$-p_1\mu_0^2 + p_3 = -q_2\mu_0\sin(\mu_0\delta) - (q_3 - q_1\mu_0^2)\cos(\mu_0\delta), \tag{4.4}$$

$$-\mu_0^3 + p_2\mu_0 > (q_3 - q_1\mu_0^2)\sin(\mu_0\delta) - q_2\mu_0\cos(\mu_0\delta). \tag{4.5}$$

Eqs. (4.4) and (4.5) are the sufficient criterion for the stability of interior equilibrium point $E^*$. We assume an upper bound $\mu_+$ on $\mu_0$ not dependent on $\delta$, such that Eq. (4.5) is satisfied for all values of $\mu$, $0 \le \mu \le \mu_+$ at $\mu = \mu_0$.

Expression (4.4) leads to

$$p_1\mu_0^2 = p_3 + q_2\mu_0\sin(\mu_0\delta) + q_3\cos(\mu_0\delta) - q_1\mu_0^2\cos(\mu_0\delta). \tag{4.6}$$

Using the bounds $|\cos(\mu_0\delta)| \le 1$, and $|\sin(\mu_0\delta)| \le 1$; Eq. (4.6) yields

$$|p_1|\mu_0^2 \le |p_3| + |q_2|\mu_0 + |q_3| + |q_1|\mu_0^2.$$

Therefore,

$$\mu_+ \le \frac{1}{2(|p_1| - |q_1|)}\left[|q_2| + \sqrt{q_2^2 + 4(|p_1| - |q_1|)(|p_3| + |q_3|)}\right], \tag{4.7}$$

also, from (4.7), $\mu_0 \le \mu_+$.

The inequality (4.5) gives us

$$\mu_0^2 < p_2 + q_2\cos(\mu_0\delta) + q_1\mu_0\sin(\mu_0\delta) - \frac{q_3\sin(\mu_0\delta)}{\mu_0}. \tag{4.8}$$

In case of $\delta = 0$, the inequality (4.8) becomes

$$\mu_0^2 < p_2 + q_2,$$

and from (4.6),

$$\begin{aligned} & p_1\mu_0^2 = p_3 + q_3 - q_1\mu_0^2 \\ \Longrightarrow\ & \mu_0^2 = \frac{p_3 + q_3}{p_1 + q_1}. \end{aligned}$$

Therefore, at $\delta = 0$, $E^*$ is asymptotically stable if $(p_3 + q_3) < (p_1 + q_1)(p_2 + q_2)$ holds.

Now, for small $\delta > 0$, from (4.6) and (4.8), we get

$$\begin{aligned} (q_3 - q_1\delta_0^2 - p_2q_2)\big[\cos(\mu_0\delta) - 1\big] + \left[(q_2 - p_1q_1)\mu_0 + \frac{p_1q_3}{\mu_0}\right]\sin(\mu_0\delta) \\ < p_1p_2 - p_3 + p_1q_2 - q_3 + q_1\mu_0^2, \end{aligned}$$

which yields

$$\begin{aligned} (q_3 - q_1\delta_0^2 - p_2q_2)\big[\cos(\mu_0\delta) - 1\big] + \left[(q_2 - p_1q_1)\mu_0 + \frac{p_1q_3}{\mu_0}\right]\sin(\mu_0\delta) \\ < (p_1 + q_1)(p_2 + q_2) - (p_3 + q_3). \end{aligned} \tag{4.9}$$

Using the bounds, we obtain

$$\begin{aligned} (q_3 - q_1\delta_0^2 - p_2q_2)\big[\cos(\mu_0\delta) - 1\big] &= 2(q_1\mu_0^2 + p_1q_2 - q_3)\sin^2\left(\frac{\mu_0\delta}{2}\right) \\ &\le \frac{1}{2}\mu_+^2|(q_1\mu_+^2 + p_1q_2 - q_3)|\delta^2, \end{aligned}$$

and

$$\left[(q_2 - p_1q_1)\mu_0 + \frac{p_1q_3}{\mu_0}\right]\sin(\mu_0\delta) \le \left[|(q_2 - p_1q_1)|\mu_+^2 + |p_1||q_3|\right]\delta_M.$$

From (4.9), we obtain that

$$\left.\begin{aligned} & \mathcal{L}_1\delta^2 + \mathcal{L}_2\delta \le \mathcal{L}_3 \\ \Longrightarrow\ & \delta_+ = \frac{1}{2\mathcal{L}_1}\left[-\mathcal{L}_2 + \sqrt{\mathcal{L}_2^2 + 4\mathcal{L}_1\mathcal{L}_3}\right], \end{aligned}\right\}$$

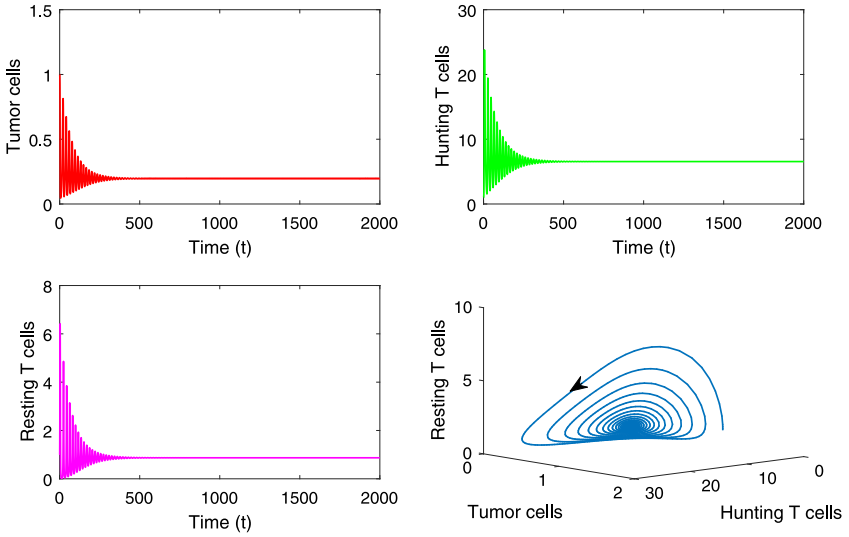


**Fig. 2.** Time series evolution curve and parametric plot of the system (2.2) around the equilibrium $E^*(0.20, 6.55, 0.87)$ for $\delta = 0.23 < 0.269$ with initial conditions $x(0) = 1$, $y(0) = 1$, $z(0) = 1$. The trajectory of the system (2.2) approaches to the stable equilibrium $E^*$.

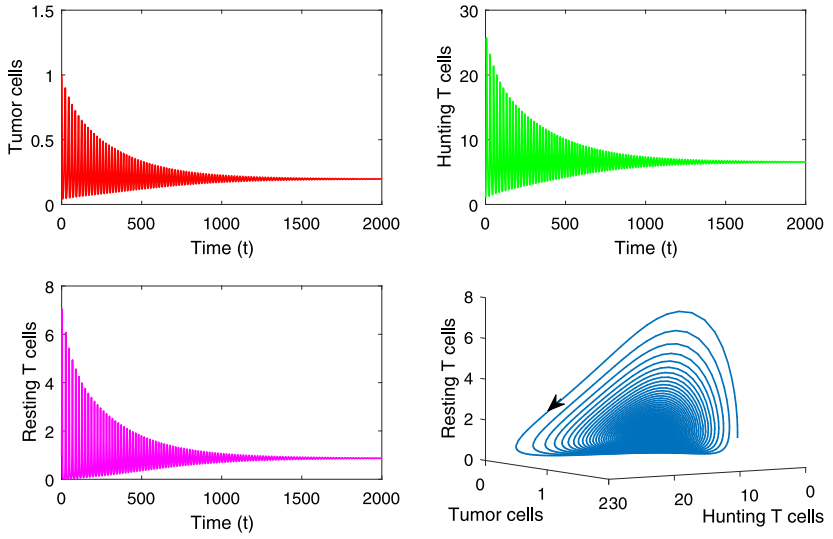


**Fig. 3.** Time series evolution curve and parametric plot of the system (2.2) around the equilibrium $E^*(0.20, 6.55, 0.87)$ for $\delta = 0.269$ with initial conditions $x(0) = 1$, $y(0) = 1$, $z(0) = 1$. The trajectory of the system (2.2) approaches to the stable equilibrium $E^*$.

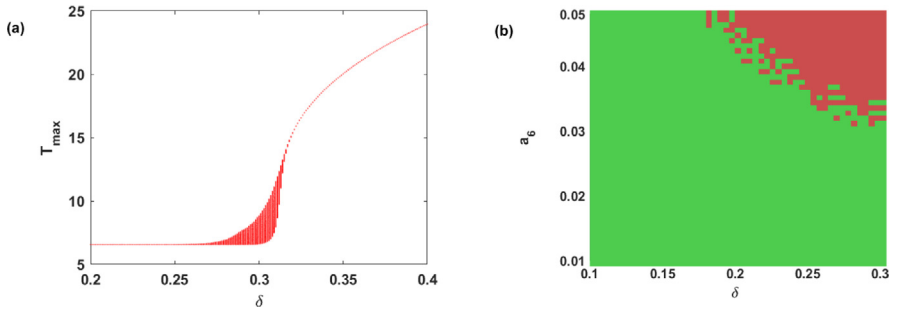


**Fig. 4.** (a) It represents $T_{max}$ vs $\delta$. Each plot is of $z$ solution component of the system (2.2). (b) It shows stability(colour:green) and instability (colour:red) region for the system (2.2). All the computations have been performed with initial condition $x(0) = 1$, $y(0) = 1$, $z(0) = 1$.

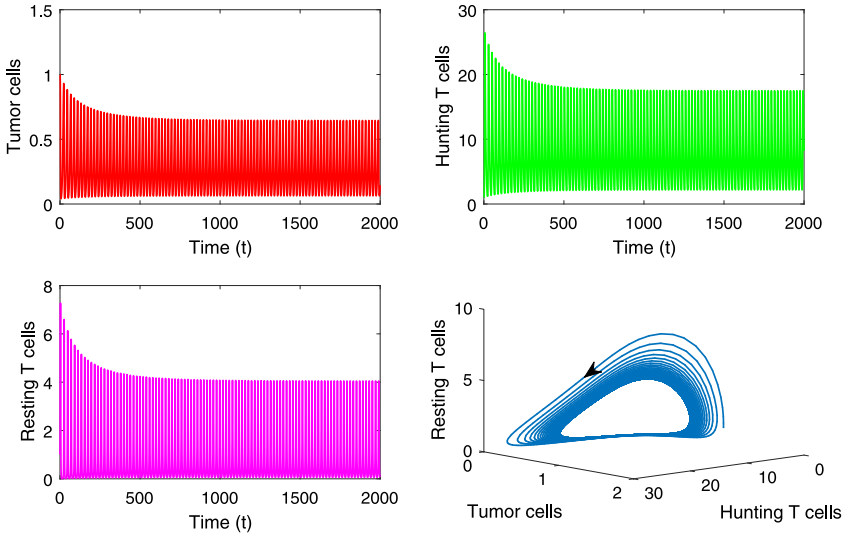


**Fig. 5.** Time series evolution curve and parametric plot of the system (2.2) around the equilibrium $E^*(0.20, 6.55, 0.87)$ for $\delta = 0.31 > 0.269$ with initial conditions $x(0) = 1,\ y(0) = 1,\ z(0) = 1$. The system (2.2) exhibits periodic oscillations and limit cycle solution.

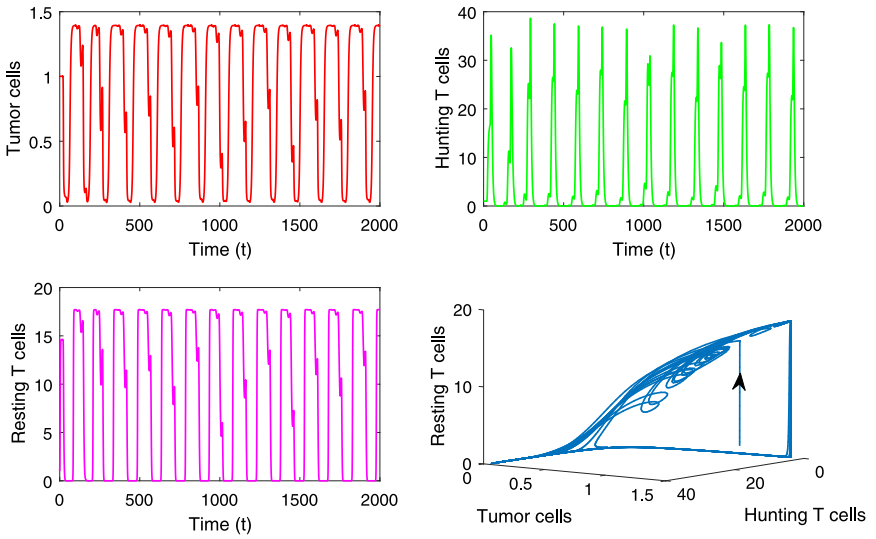


**Fig. 6.** Time series evolution curve and parametric plot of the system (2.2) around the equilibrium $E^*(0.20, 6.55, 0.87)$ for $\delta = 20 \gg 0.269$ with initial conditions $x(0) = 1,\ y(0) = 1,\ z(0) = 1$. The system (2.2) initiates aperiodic behaviour and unstable nature.

where,

$$\mathcal{L}_1 = \frac{1}{2}|(q_1\mu_+^2 + p_1q_2 - q_3)|\mu_+^2,$$
$$\mathcal{L}_2 = \left[|(q_2 - p_1q_1)|\mu_+^2 + |p_1||q_3|\right],$$
$$\mathcal{L}_3 = (p_1 + q_1)(p_2 + q_2) - (p_3 + q_3).$$

Hence, the Nyquist criterion holds if $0 \leq \delta \leq \delta_+$, and the periodic solution preserves the limit cycle's stability for the maximum length of time lag $\delta_+$.

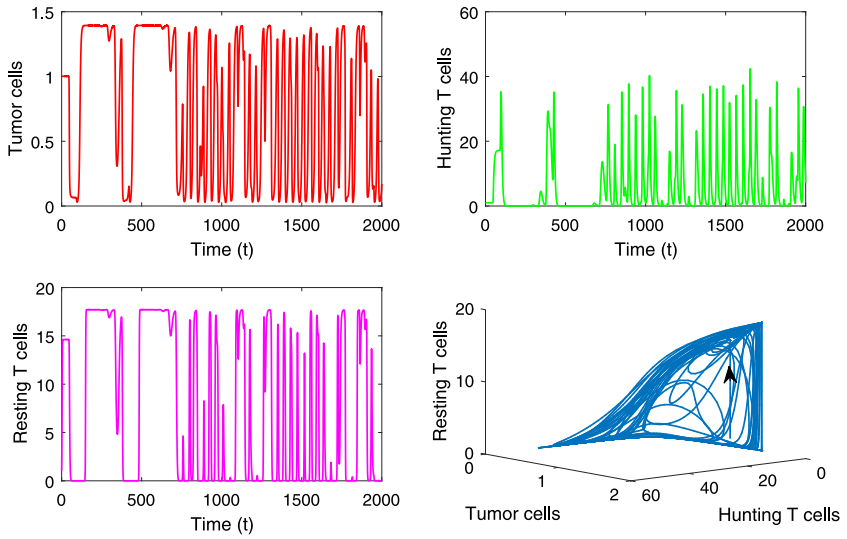


**Fig. 7.** Time series evolution curve and parametric plot of the system (2.2) around the equilibrium $E^*(0.20, 6.55, 0.87)$ for $\delta = 45 \gg 0.269$ with initial conditions $x(0) = 1,\ y(0) = 1,\ z(0) = 1$. The system (2.2) initiates more aperiodic behaviour and unstable nature.

## 5. Numerical simulation

Based on the above theoretical outcomes, we will present some numerical computations of the proposed tumour model in this section. We define the parameters and units arbitrarily, as used in Refs. [25]. At first, we investigate the dynamics of the model with the variation of a discrete-time lag $\delta$. For this purpose, we consider the parameter set as: $a_1 = 1.82$, $a_2 = 0.239$, $a_3 = 0.2$, $a_4 = 0.04$, $a_5 = 0.0691$, $a_6 = 0.05$, $a_7 = 0.01$, $a_8 = 2$, and $K = 1$. Considering the mentioned parameter set, we found three biologically feasible equilibrium points: $E_1(1.39, 0, 0)$, $E_2(1.39, 0, 17.70)$, and $E^*(0.20, 6.55, 0.87)$. The eigenvalues corresponding to the equilibrium $E_1$ are $-3.24$, $-0.26$, and $1.22$. Hence, $E_1$ is a point of unstable saddle type. The equilibrium $E_2$ has eigenvalues of $-3.24$, $3.98$, and $-1.22$; which correspond to an unstable saddle point. For $\delta = 0$ the eigenvalues correspond to interior equilibrium $E^*$ are $-5.48$, $-0.016 \pm 0.37\iota$; which suggests that $E^*$ is a stable inward spiral. For $\delta \neq 0$, the stability of $E^*$ depends on $\kappa_1$, $\kappa_2$, $\kappa_3$ and $\omega$. For the set of parameters $a_1 = 1.82$, $a_2 = 0.239$, $a_3 = 0.2$, $a_4 = 0.04$, $a_5 = 0.0691$, $a_6 = 0.05$, $a_7 = 0.01$, $a_8 = 2$, $K = 1$; the value of $\kappa_1 = 29.77 > 0$, $\kappa_2 = -0.154 < 0$, and $\kappa_3 = -0.46 < 0$. Therefore, Eq. (3.7) has a unique positive real root $\omega_0 \approx 0.36$; hence Eq. (3.8) yields $\delta_0 \approx 0.2693$. It is also confirmed that the transversality condition for Hopf bifurcation $\frac{d(Re(m))}{d\delta}|_{\delta=\delta_0,\omega=\omega_0} = 11.38 > 0$, which guarantees the occurrence of Hopf bifurcation at $\delta_0 = 0.269$. Thus, from Proposition 4.1, we can achieve a Hopf bifurcation at $\delta_0 = 0.269$ for the model (2.2) and the equilibrium $E^*$ is stable for $0 \leq \delta < 0.269$. These two situations can be observed from Fig. 2 for $\delta = 0.23 < 0.269$ and Fig. 3 for $\delta_0 = 0.269$. The stability of model (2.2) changes as time-delay $\delta$ crosses the threshold value $\delta_0 \approx 0.269$, and system (2.2) exhibits regular periodic oscillations to irregular long periodic oscillations. Fig. 5 illustrates that for $\delta = 0.31 > 0.269$, there exist regular periodic oscillations for the system (2.2) corresponds to the initiation of a limit cycle. Fig. 6 for $\delta = 20$ and Fig. 7 for $\delta = 45$ demonstrates that for large values of delay $\delta$, the system (2.2) shows chaotic like nature with an irregular pattern of each cell population. We have also calculated the length of the maximum time lag $\delta_+ \approx 0.61$ for which the system (2.2) preserves the limit cycle solution.

The discussions that have taken place above are extremely interesting and relevant in real life from a biological standpoint. If the growth process of hunting T-cells in the patient's body increases gradually, the immune system can stabilize the growth of tumour cells. If there is only a slight delay in the growth process, the patient's immune system can still control the growth of tumour cells. However, after a certain amount of time has passed, all three cells compete with one another, resulting in a Hopf bifurcation. Despite this, because of the significant delay in the growth process, the patient's immune system will not control tumour growth, and the patient's condition will deteriorate further.

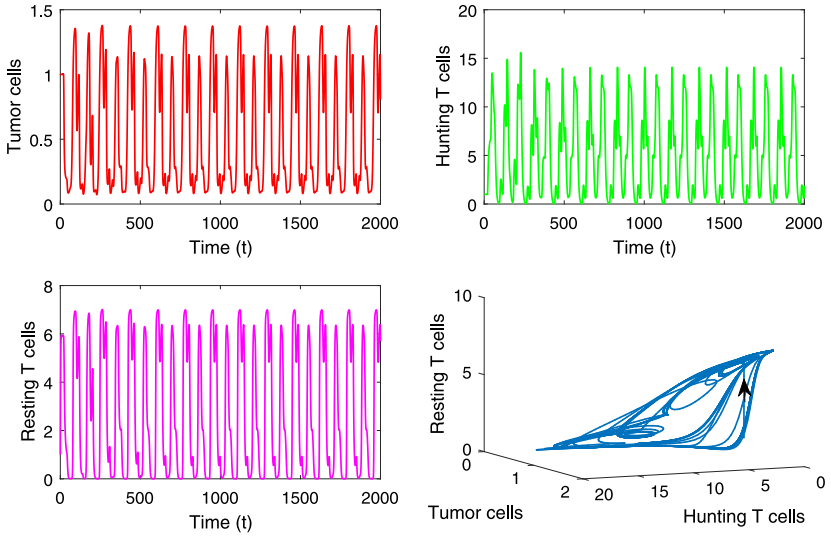


**Fig. 8.** Time series solution and parametric plot of the system (2.2) for $a_5 = 0.191$ with initial conditions $x(0) = 1$, $y(0) = 1$, $z(0) = 1$. The system (2.2) exhibits irregular periodic oscillations and unstable solution.

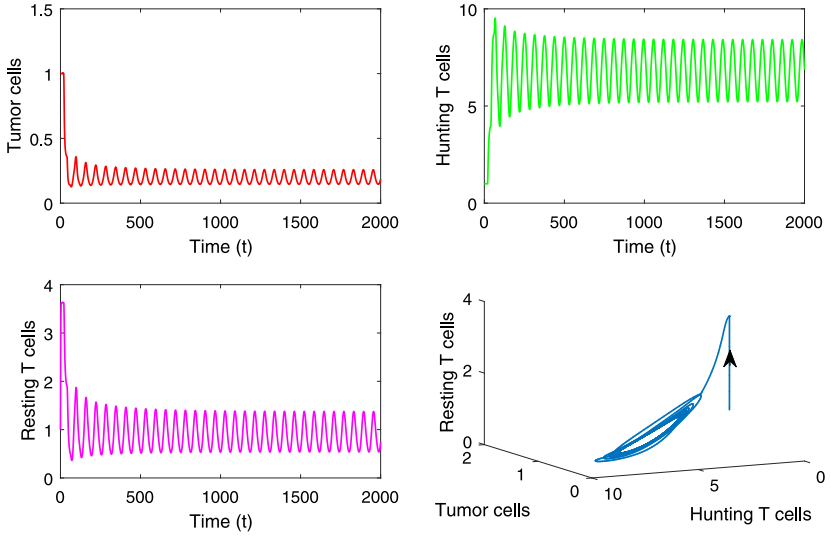


**Fig. 9.** Time series solution and parametric plot of the system (2.2) for $a_5 = 0.358$ with initial conditions $x(0) = 1$, $y(0) = 1$, $z(0) = 1$. The system (2.2) exhibits periodic oscillations and limit cycle solution.

Fig. 4 presents Hopf-bifurcation of the $z$-solution component of the system (2.2) with respect to the bifurcating parameter $\delta$ and the stability region is given under $(\delta, a_5) \in [01., 0.3] \times [0.01, 0.05]$. In the bifurcation diagram, it can be observed that the dynamics of the system (2.2) changes from a stable-to-unstable state and then to a stable state.

Now, we consider a patient with a time-delay in the growth process of hunting T-cells $\delta = 20 > 0.269$. We fixed the other parameters as $a_1 = 1.82$, $a_2 = 0.239$, $a_3 = 0.2$, $a_4 = 0.04$, $a_6 = 0.05$, $a_7 = 0.01$, $a_8 = 2$, $K = 1$ and varied the growth rate of resting T-cells, i.e., the parameter $a_5$. It is clearly observed from Fig. 6, with $a_5 = 0.0691$ and $\delta = 20$, the system (2.2) shows irregular long periodic oscillations, i.e., the patients' condition is unstable.

Fig. 8 demonstrates that if the growth rate of resting T-cells $a_5 = 0.191$, the system is still unstable and aperiodic.

From Fig. 9, if the patient's body has the growth rate of resting T-cells $a_5 = 0.358$ then regular periodic solutions occurs for the system (2.2) which indicates that the initiation of limit cycles.

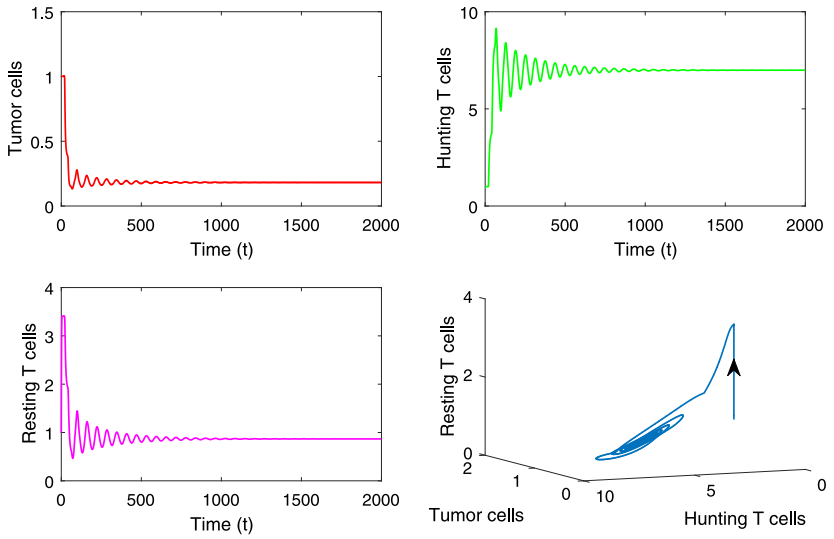


**Fig. 10.** Time series solution and parametric plot of the system (2.2) for $a_5 = 0.391$ with initial conditions $x(0) = 1$, $y(0) = 1$, $z(0) = 1$. The system (2.2) undergoes a stable position through an inward spiral.

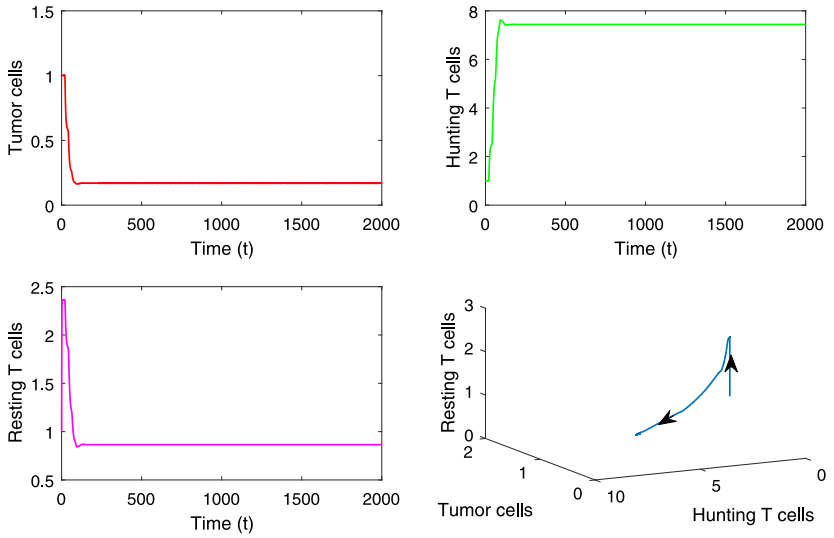


**Fig. 11.** Time series solution and parametric plot of the system (2.2) for $a_5 = 0.691$ with initial conditions $x(0) = 1$, $y(0) = 1$, $z(0) = 1$. The system (2.2) converges to stable position.

It can be observed from Fig. 10 that if the growth rate of resting T-cells is increased, i.e., if $a_5 = 0.391$, then the immune system can control the tumour growth, and the body becomes stable.

Fig. 11 shows that if the patient's body has a high growth rate of resting T-cells, i.e., $a_5 = 0.691$ then it assures that the immune system is strong enough to suppress the tumour growth at the very initial stage and that the body gets back to a healthy condition.

## 6. Conclusion

This study has proposed a prey–predator type nonlinear time-delay system consisting of three cell populations, namely tumour cells, hunting $T$ cells, and resting $T$ cells, to describe the effect of discrete-time delayed in tumour–immune interactions. At each equilibrium point of the system, linear stability analyses have been performed, and

the results show that the system undergoes a Hopf bifurcation under the effect of time delay. The system is also reported to show periodic solutions for a specific time delay, indicating the existence of limit cycles. The biological point of view reveals that the continuous growth process of hunting T-cells is beneficial for the immune system to stabilize tumour growth. Furthermore, a smaller delay in the growth process does not affect the system's stability, and the immune system still controls tumour growth. However, the system loses stability when, after a significant delay, all three cells begin competing, resulting in a Hopf bifurcation. The growth rate of resting T-cells has also been simulated numerically by varying the parameter $a_5$. By increasing the value of the parameter $a_{[5]}$, the system shows stable behaviour. The study suggests that resting T-cell growth is also critical for stabilizing tumour cells. A primary limitation of our paper is that we assumed theoretical parameter values in our numerical simulations. However, medical data can be used to verify our theoretical results. Furthermore, the model can be extended to a more nonlinear one by taking the conversion term of hunting T-cells to resting T-cells as a Michaelis–Menten kinetic response.

## Declaration of competing interest

The authors declare that they have no known competing financial interests or personal relationships that could have appeared to influence the work reported in this paper.

## References

[1] I. Abdulrashid, A.A.M. Alsammani, X. Han, Stability analysis of a chemotherapy model with delays, Discrete Contin. Dyn. Syst. Ser. B 24 (3) (2019) 989–1005, http://dx.doi.org/10.3934/dcdsb.2019002.
[2] S. Ahmad, A. Ullah, A. Akgül, D. Baleanu, Analysis of the fractional tumour-immune-vitamins model with Mittag–Leffler kernel, Results Phys. 19 (2020) 103559, http://dx.doi.org/10.1016/j.rinp.2020.103559.
[3] S.A. Alharbi, A.S. Rambely, A new ODE-based model for tumour cells and immune system competition, Mathematics 8 (2020) 1285, http://dx.doi.org/10.3390/math8081285.
[4] S. Banerjee, R.R. Sarkar, Delay-induced model for tumour–immune interaction and control of malignant tumour growth, BioSystems 91 (2008) 268–288, http://dx.doi.org/10.1016/j.biosystems.2007.10.002.
[5] R.J. Beck, B. Weigelin, J.B. Beltman, Mathematical modelling based on in vivo imaging suggests CD137-stimulated cytotoxic T-lymphocytes exert superior tumour control due to an enhanced antimitotic effect on tumour cells, Cancers 31 (2021) 2567, http://dx.doi.org/10.3390/cancers13112567.
[6] P. Bi, H. Xiao, Bifurcations of tumour-immune competition systems with delay, Abstr. Appl. Anal. (2014) 723159, http://dx.doi.org/10.1155/2014/723159.
[7] Q. Dai, Co-dimension two bifurcations analysis of a delayed tumor model with Allee effect, Adv. Differ. Equ. 2021 (2021) 516.
[8] P. Das, P. Das, Effects of delayed immune-activation in the dynamics of tumor-immune interactions math, Model. Nat. Phenom. 15 (45) (2020).
[9] P. Das, P. Das, S. Das, An investigation on monod-haldane immune response based tumour-effectorinterleukin-2 interactions with treatments, Appl. Math. Comput. 361 (2021) 536–551.
[10] P. Das, S. Das, P. Das, F.A. Rihan, M. Uzuntarla, D. Ghosh, Optimal control strategy for cancer remission using combinatorial therapy: A mathematical model-based approach, Chaos, Solitons Fractal 145 (2021) 110789.
[11] P. Das, P. Das, S. Mukherjee, Stochastic dynamics of Michaelis-Menten kinetics based tumour-immune interactions, Physica-A 541 (2019) 123603.
[12] P. Das, S. Das, R.K. Upadhyay, P. Das, Optimal treatment strategies for delayed cancer-immune system with multiple therapeutic approach, Chaos Solit. Fractals 136 (2020) 109806, http://dx.doi.org/10.1016/j.chaos.2020.10980.
[13] P. Das, P. Mondal, P. Das, T.K. Roy, Stochastic persistence and extinction in tumor-immune system perturbed by white noise, Int. J. Dyn. Control. 10 (2021) 620–629.
[14] P. Das, Sayan Mukherjee, P. Das, An investigation on Michaelis - Menten kinetics based complex dynamics of tumour - immune interaction, Chaos, Solitons Fractal 128 (2019) 297–305.
[15] P. Das, S. Mukherjee, P. Das, S. Banerjee, Characterizing chaos and multifractality in noise-assisted tumour-immune interplay, Nonlinear Dyn. 101 (1) (2021) 675–685.
[16] P. Das, R.K. Upadhyay, P. Das, D. Ghosh, Exploring dynamical complexity in a time-delayed tumour-immune model, Chaos 30 (12) (2021) 123118.
[17] L.G. de Pillis, A.E. Radunskaya, C.L. Wiseman, A validated mathematical model of cell-mediated immune response to tumour growth, Cancer Res. 65 (17) (2005) 7950–7958, http://dx.doi.org/10.1158/0008-5472.CAN-05-0564.
[18] K. Dehingia, H.K. Sarmah, Y. Alharbi, K. Hosseini, Mathematical analysis of a cancer model with time-delay in tumour-immune interaction and stimulation processes, Adv. Difference Equ. 2021 (2021) 473, http://dx.doi.org/10.1186/s13662-021-03621-4.
[19] Y. Dong, G. Huang, R. Miyazaki, Y. Takeuchi, Dynamics in a tumour immune system with time-delays, Appl. Math. Comput. 252 (2015) 99–113, http://dx.doi.org/10.1016/j.amc.2014.11.096.
[20] Y. Dong, R. Miyazaki, Y. Takeuchi, Mathematical modeling on helper T-cellss in a tumour immune system, Discrete Continuous Dyn. Syst. Ser. B 19 (1) (2014) 55–72, http://dx.doi.org/10.3934/dcdsb.2014.19.55.

[21] H. Dritschel, S.L. Waters, A. Roller, H.M. Byrne, A mathematical model of cytotoxic and helper $T$ cell interactions in a tumour microenvironment, Lett. Biomath. 5 (sup1) (2018) S36–S68, http://dx.doi.org/10.1080/23737867.2018.1465863.
[22] A. El-Gohary, Chaos and optimal control of cancer self-remission and tumour system steady states, Chaos Solitons Fractals 37 (2008) 1305–1316, http://dx.doi.org/10.1016/j.chaos.2006.10.060.
[23] H.I. Freedman, V.S.H. Rao, The trade-off between mutual interference and time lag in predator–prey systems, Bull. Math. Biol. 45 (6) (1983) 991–1004.
[24] D. Ghosh, S. Khajanchi, S. Mangiarotti, F. Denis, S.K. Dana, C. Letellier, How tumour growth can be influenced by delayed interactions between cancer cells and the microenvironment? BioSystems 158 (2017) 17–30, http://dx.doi.org/10.1016/j.biosystems.2017.05.001.
[25] G. Kaur, N. Ahmad, On study of immune response to tumour cells in prey-predator system, Int. Sch. Res. Not. (2014) 346597, http://dx.doi.org/10.1155/2014/346597.
[26] S. Khajanchi, M. Perc, D. Ghosh, The influence of time-delay in a chaotic cancer model, Chaos: Interdiscip. J. Nonlinear Sci. 28 (10) (2018) 103101, http://dx.doi.org/10.1063/1.5052496.
[27] V.A. Kuznetsov, L.A. Makalkin, M.A. Taylor, A.S. Perelson, Nonlinear dynamics of immunogenic tumours: Parameter estimation and global bifurcation analysis, Bull. Math. Biol. 56 (2) (1994) 295–321.
[28] P. Liu, X. Liu, Dynamics of a tumour-immune model considering targeted chemotherapy, Chaos Solit. Fractals 98 (2017) 7–13.
[29] D. Liu, S. Ruan, D. Zhu, Stable periodic oscillations in a two-stage cancer model of tumour and immune system interactions, Math. Biosci. Eng. 9 (2012) 347–368.
[30] J. Malinzi, K.B. Basita, S. Padidar, H.A. Adeola, Prospect for application of mathematical models in combination cancer treatments, Info. Med. Unlocked 23 (2021) 100534, http://dx.doi.org/10.1016/j.imu.2021.100534.
[31] H.N. Moore, N.K. Li, A mathematical model for chronic myelogenous leukemia (CML) and T-cells interaction, J. Theoret. Biol. 227 (2004) 513–523.
[32] H. Nyquist, Regeneration theory, Bell. Syst. Tech. J. 11 (1) (1932) 126–147.
[33] L. Pang, S. Liu, X. Zhang, T. Tian, Mathematical modelling and dynamic analysis of anti-tumour immune response, J. Appl. Math. Comput. 62 (2020) 473–488, http://dx.doi.org/10.1007/s12190-019-01292-9.
[34] F.A. Rihan, Delay Differential Equations and Applications to Biology, first ed., Springer, 2021.
[35] F.A. Rihan, D.H.A. Rahman, S. Lakshmanan, A.S. Alkhajeh, A time-delay model of tumour–immune system interactions: Global dynamics, parameter estimation, sensitivity analysis, Appl. Math. Comput. 232 (2014) 606–623, http://dx.doi.org/10.1016/j.amc.2014.01.111.
[36] F.A. Rihan, M. Safan, M.A. Abdeen, D.A. Rahman, Qualitative and computational analysis of a mathematical model for tumour-immune interactions, J. Appl. Math. (2012) 475720, http://dx.doi.org/10.1155/2012/475720.
[37] M. Saleem, T. Agrawal, Chaos in a tumour growth model with delayed response of the immune system, J. Appl. Math. (2012) 891095, http://dx.doi.org/10.1155/2012/891095.
[38] M. Sardar, S. Khajanchi, S. Biswas, S.F. Abdelwahab, K.S. Nisar, Exploring the dynamics of a tumour-immune interplay with time-delay, Alex. Eng. J. 60 (2021) 4875–4888, http://dx.doi.org/10.1016/j.aej.2021.03.041.
[39] R.R. Sarkar, S. Banerjee, Cancer self remission and tumour stability–A stochastic approach, Math. Biosci. 196 (2005) 65–81, http://dx.doi.org/10.1016/j.mbs.2005.04.001.
[40] Y. Shu, J. Huang, Y. Dong, Y. Takeuchi, Mathematical modeling and bifurcation analysis of pro- and anti-tumour macrophages, Appl. Math. Model. (2020) http://dx.doi.org/10.1016/j.apm.2020.06.042.
[41] P.A. Valle, L.N. Coria, C. Plata, Personalized immunotherapy treatment strategies for a dynamical system of chronic myelogenous leukemia, Cancers 13 (2021) 2030, http://dx.doi.org/10.3390/cancers13092030.
[42] J. Wang, Y. Zhang, Dynamics of immunotherapy antitumor models with impulsive control strategy, Math. Methods Appl. Sci. 45 (2022) 483–499.
[43] X. Yang, L. Chen, J. Chen, Permanence and positive periodic solution for the single-species nonautonomous delay diffusive model, Comput. Math. Appl. 32 (4) (1996) 109–116.
[44] Z. Yang, C. Yang, Y. Dong, Y. Takeuchi, Mathematical modelling of the inhibitory role of regulatory T cells in tumor immune response, Complexity 2020 (2020) 4834165.
[45] T.A. Yildiz, S. Arshad, D. Baleanu, Optimal chemotherapy and immunotherapy schedules for a cancer-obesity model with Caputo time fractional derivative, Math. Methods Appl. Sci. 41 (18) (2018) 9390–9407, http://dx.doi.org/10.1002/mma.5298.